A data-driven approach for fatigue-based individual blade pitch controller selection from wind conditions

David Collet, Domenico Di Domenico, Guillaume Sabiron, Mazen Alamir

A data-driven approach for fatigue-based individual blade pitch controller selection from wind conditions

David Collet[1,2], Domenico Di Domenico[1], Guillaume Sabiron[1] and Mazen Alamir[2]

***Abstract*— In a context of wind power production growth, it is necessary to optimize the levelized cost of energy by reducing the wind turbine operation and maintenance costs. This paper addresses these issues through an innovative data-driven approach, applied to individual pitch control and based on wind conditions clustering, from light detection and ranging (LiDAR) wind field reconstruction. A set of controllers is first designed, and a surrogate model is fitted to predict the economic fatigue cost of the wind turbine in closed-loop for each of these controllers, given a cluster of wind conditions. This allows on-line selection of the controller minimizing mechanical fatigue loads among the candidates for each wind condition. Preliminary tests show promising results regarding the effectiveness of this method in reducing wind turbine fatigue when compared to a single optimized individual pitch controller. The main advantages of this approach are to limit the sensitivities to controller tuning procedure and to provide an economically driven control strategy based on fatigue theory that can be effectively adapted to different wind turbine systems.**

I. INTRODUCTION

Wind energy production has been exponentially growing in the last decades, with about 539 GW globally installed in 2017 compared with 94 GW in 2007 [1]. In order to achieve COP21 objective, which is to maintain CO_2 emissions below 5.4×10^{12} kilogram per year, the wind energy industry is expected to develop even further [2]. This energetic transition represents a large economic investment. It is thus necessary to optimize Horizontal Axis Wind Turbine (HAWT) operation and maintenance cost. Control of HAWT blade pitch angle can contribute to this issue.

The main objectives of HAWT blade pitch control are to regulate output power, rotor speed and minimize mechanical strains. A classical assumption is that wind is uniformly distributed over the rotor area. Therefore, all the blades are pitched to the same angle, this technique is called Collective Pitch Control (CPC). With recent increase in rotor diameter, the assumption is less and less valid. Aerodynamic forces on the blades fluctuate with the azimuth angle while the pitch angle remains constant [3]. Therefore, by varying each blade pitch angle individually depending on its azimuth, blades fatigue loads can be alleviated. This technique is called Individual Pitch Control (IPC) [4].

In the literature, works on IPC begin with basic control strategies like Proportional Integral (PI) control [4] and are followed by more advanced ones such as linear quadratic regulator [4], H_∞ control [5], Model Predictive Control (MPC) [6], Non linear MPC (NMPC) [7], fuzzy logic [8] or linear parameter varying control [9]. The direct expression of fatigue reduction, using the Palmgrem-Miner fatigue theory [10] in optimal control techniques is not straightforward [11], [12] and remains an open topic [13]. Therefore, the fatigue reduction objective is indirectly formulated, using a quadratic cost function [13]. However, quadratic cost functions do not allow to quantify the fatigue [13], which is important for weighting trade-offs among the damages of various HAWT components.

Furthermore, since wind is the main exogenous variable acting on the HAWT system, turbulent spectrum characteristics and HAWT closed loop dynamics are the two major parameters influencing HAWT fatigue cost. Moreover, wind turbulent spectrum characteristics on a given site can vary significantly over two hours due to diurnal and synoptic variations [14], but also atmospheric conditions (e.g. temperature stratification) [15]. These variations allow the clusterization of the wind based on its spectrum characteristics and corresponding atmospheric conditions [15]. Wind Field Reconstruction (WFR) algorithms [16] have allowed to estimate many of the wind spectrum features necessary for the wind definition. Works related to HAWT fatigue prediction from wind characteristics for predictive maintenance or site assessment [17], [18], [19], [20], [21] have shown that it is possible to accurately predict fatigue loads from wind spectrum features. The most performing WFR algorithms are based on Light Detection And Ranging (LiDAR), which is a technique using the Doppler principle to remotely measure aerosols velocity in the air with laser beams.

In this paper, an innovative data-driven framework is presented, minimizing directly HAWT fatigue cost by using a discrete set of blade pitch candidate controllers. The key of this method is a surrogate model relating the triplets wind spectrum features, controller and fatigue cost. Thanks to this surrogate model, assuming that an estimation of the current wind spectrum features can be obtained using LiDAR measurements and WFR algorithms, the fatigue cost associated to each controller can be estimated. Therefore, the controller minimizing the fatigue cost for the current wind is selected on-line for closed loop regulation of the HAWT.

The paper is organized as follows. In Section II the holistic concept is detailed. Then, the design steps of this framework are illustrated through an application, presented in Section III. The results of this application are presented in Section IV and eventually the conclusion is given in

[1]IFP Energies nouvelles Lyon, Rond-point de l'échangeur de Solaize, 69360 Solaize, France

[2]GIPSA-lab, CNRS, University of Grenoble-Alpes, France

Section V.

II. HOLISTIC CONCEPT

To decide on-line which controller gives the lowest HAWT fatigue cost in closed loop among a discrete set of candidate controllers, a fatigue based cost function assessing controller economic performance is designed. This cost function uses, for damage estimation, the widely accepted Palmgrem-Miner fatigue theory [10], further detailed in Section III-D.1. Unlike quadratic cost functions, the Palmgrem-Miner theory allows one to accurately quantify the damage on each HAWT component [13]. To avoid the computationally expensive prediction of HAWT fatigue from inflow wind using physical laws, a data-driven surrogate model appears to be a promising solution for predicting fatigue in an acceptable computational time [21].

The design of this framework is divided into five steps:

1) A set of m candidate controllers, denoted by $\mathcal{K}_{\text{list}} = \{K_1, ..., K_m\}$ must be designed, where K_j is the candidate controller j. Each controller in $\mathcal{K}_{\text{list}}$ must ensure the proper regulation of the closed loop HAWT.
2) Data are generated by running simulations of a HAWT in closed loop with each candidate controller, under a set of winds coming from a numerical wind generator or a LiDAR measurement campaign. The point of the data generation process is to gather triplets of wind time series, HAWT outputs time series and corresponding controller.
3) Turbulent wind spectrum features are extracted from the wind time series w, yielding the wind features column vector X which defines the wind. These wind features vectors are rearranged to form the wind features space $\mathcal{X} = \{X_1, ..., X_n\}$.
4) HAWT outputs time series are evaluated using the fatigue based cost function to yield the target value mapping $\mathcal{Y}$. The target value mapping is defined such that $\mathcal{Y}(X_i, K_j)$ is the fatigue cost of the HAWT in closed loop with the controller $K_j \in \mathcal{K}_{\text{list}}$, under the wind defined by the wind features vector $X_i \in \mathcal{X}$.
5) The surrogate model, denoted by f, must be designed to predict the fatigue cost associated to a wind features vector X_i and the HAWT in closed loop with a controller $K_j \in \mathcal{K}_{\text{list}}$. It is fitted on the generated data and thus:

$$f(X_i, K_j) \simeq \mathcal{Y}(X_i, K_j) \tag{1}$$

A possible on-line implementation is depicted in Fig. 1. From the wind features vector X obtained from LiDAR measurements and WFR algorithm, the surrogate model f predicts the fatigue cost for each candidate controller in $\mathcal{K}_{\text{list}}$. Then the Selector selects the controller $K^* \in \mathcal{K}_{\text{list}}$ minimizing the cost function for the current wind conditions, based on the surrogate model f fatigue cost predictions:

$$K^*(X, f, \mathcal{K}_{\text{list}}) = \underset{K_j \in \mathcal{K}_{\text{list}}}{\operatorname{argmin}} f(X, K_j) \tag{2}$$

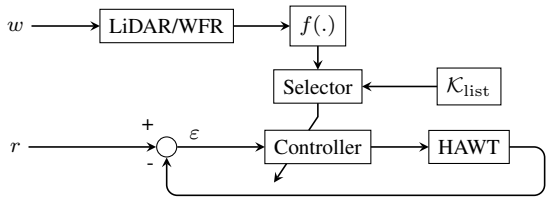

Fig. 1: On-line implementation of the controller selection framework. r refers to the set point, ε to the regulation error and w is the wind.

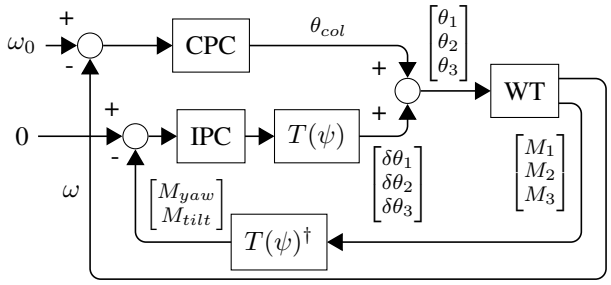

Fig. 2: Wind turbine blade pitch control system scheme, with independent IPC and CPC controllers. ω refers to the rotational speed and ω_0 to its set point. θ_{col} is the collective pitch angle, $\delta\theta_i$ is the pitch angle variation of blade i and θ_i is the pitch angle set-point of blade i.

III. APPLICATION

In this section, an application of this framework is presented as an example. It should be noticed that in the sequel nor the candidate controllers, the features extracted from wind time series and the surrogate model are fixed. These are only blocks of the framework, that the user can fill with any suitable controller or surrogate model. There is a wide range of combinations possibilities and finding the optimal one is out of the scope of this study. The outline of this section follows the design steps of the framework presented in Section II. In Subsection III-A the set of candidate controllers design is shown and the data generation process is depicted in Subsection III-B. The wind spectrum features extracted from wind time series are presented in Subsection III-C, the cost function evaluating HAWT fatigue cost is defined in Subsection III-C and in Subsection III-E the design of the surrogate model is described.

A. Candidate controllers design

In this application, IPC controllers in addition to a CPC controller are considered (Fig. 2). The CPC controller corresponds to a PI controller, gain scheduled on blade pitch angle, designed as in [22]. The IPC controllers design is explained in the sequel.

The usual IPC approach is to transform the pitch angles variations and blade root bending moments, expressed in a rotating coordinate system, to a non-rotating one. This transformation is achieved using the Coleman transform matrix $T(\psi)$ [23]:

TABLE I: HAWT characteristics summary.

Characteristics	Value
Rated Power (kW)	2050
Cut-in speed (m/s)	3.5
Rated speed (m/s)	14.5
Cut-off speed (m/s)	25
Rotor diameter (m)	82
Rotor speed (rpm)	8.5 — 17.1

TABLE II: Wind spectrum parameters variation.

Parameter	Set of values
Wind speed (m/s)	$\{10, 12, 14, 16, 18, 20, 22\}$
Wind direction (deg.)	$\{-15, -10, -5, 0, 5, 10, 15\}$
Turbulence class	$\{A, B, C\}$

$$T(\psi) = \begin{pmatrix} \cos(\psi) & \sin(\psi) \\ \cos(\psi + \frac{2\pi}{3}) & \sin(\psi + \frac{2\pi}{3}) \\ \cos(\psi + \frac{4\pi}{3}) & \sin(\psi + \frac{4\pi}{3}) \end{pmatrix} \quad (3)$$

where ψ is the azimuth angle of blade 1. By matrix multiplication with the IPC controller outputs, namely the vertical and horizontal pitch angles in the non-rotating coordinate system, the blade pitch angle variations of blades 1, 2 and 3, denoted by $\delta\theta_1$, $\delta\theta_2$ and $\delta\theta_3$, are obtained. Conversely the Moore-Penrose pseudo-inverse of $T(\psi)$, denoted by $T(\psi)^\dagger = \left(T(\psi)^T T(\psi)\right)^{-1} T(\psi)^T = \frac{2}{3} T(\psi)^T$, is used to estimate the rotor vertical and horizontal unbalanced loads, denoted by M_{yaw} and M_{tilt}, from the measured blade root bending moments M_1, M_2 and M_3. The IPC controller considered here is a double single input single output PI and its objective is to regulate rotor unbalanced loads toward zero.

The CPC parameters are fixed, while the proportional and integral gains, respectively denoted by K_P and K_I, are varied to generate a grid of one hundred controllers.

B. Data generation process

Data are generated using an aero-elastic HAWT simulator. The HAWT used for data generation is a Senvion MM82 whose technical characteristics are summarized in Table I, simulated with the NREL aero elastic HAWT simulator FAST [24] under full-field turbulent wind time series.

For the simulations, FAST was sampled at 80 Hz with blade 1^{st} edgewise, 1^{st} and 2^{nd} flapwise, drivetrain rotational-flexibility, generator, yaw, tower 1^{st} and 2^{nd} fore-aft and side-side degrees of freedom activated.

Wind time series are generated with NREL wind generator TurbSim [25], by imposing a Kaimal spectrum. The wind spectrum parameters for the wind set generation are summarized in Table II, every parameter combination is generated with 4 different random seeds, giving 588 winds. The turbulence class corresponds to the standard IEC (International Electrochemical Commission) 61400-1 categories of turbulence [26], with 'A' being the most turbulent.

In this application, the HAWT is simulated in closed loop with each candidate controller under every wind time series.

C. Wind features extraction

In order to have high fatigue cost prediction accuracy, wind characteristics likely to explain wind turbine fatigue variance are needed. WFR algorithms allow to estimate at time t, characteristics of the two dimensional wind velocity field at the rotor plane from LiDAR measurements. $\overrightarrow{V}(t, y, z) = [u(t, y, z), v(t, y, z), w(t, y, z)]^T$ is the three dimensional velocity vector at horizontal position y and vertical position z. Let $V(t, y, z)$ be the euclidean norm of $\overrightarrow{V}(t, y, z)$. The considered wind characteristics are the mean and standard deviation over the simulation duration, from t_0 to t_f, of the Rotor Averaged Wind Speed (RAWS) (4a), horizontal and vertical shear denoted by δ_y (4b) and δ_z (4c), tilt and yaw misalignment denoted by θ_y (4d) and θ_z (4e) for a total of ten features. Moreover an additional feature, namely the Rotor Averaged Turbulence Intensity (RATI), is considered on the same period. Note that RATI is already averaged over time. The wind features vector is therefore of dimension eleven. To summarize, the wind characteristics are:

$$\mathrm{RAWS}(t) = \frac{1}{S}\int_S V ds \quad (4a)$$

$$\delta_y(t) = \frac{1}{S}\int_S \frac{\partial V}{\partial y} ds \quad (4b)$$

$$\delta_z(t) = \frac{1}{S}\int_S \frac{\partial V}{\partial z} ds \quad (4c)$$

$$\theta_y(t) = \frac{1}{S}\int_S \arctan\left(\frac{w}{u}\right) ds \quad (4d)$$

$$\theta_z(t) = \frac{1}{S}\int_S \arctan\left(\frac{v}{u}\right) ds \quad (4e)$$

$$\mathrm{RATI} = \frac{1}{S}\int_S \frac{\int_{t_0}^{t_f} V^2 dt - \left(\int_{t_0}^{t_f} V dt\right)^2}{\int_{t_0}^{t_f} V dt} ds \quad (4f)$$

where S is the rotor area and $ds = dydz$ is an infinitesimal area of the rotor. It should be noticed that these features can be obtained using WFR algorithm and LiDAR measurements.

D. Fatigue based cost function evaluation

1) Fatigue theory: It is possible to estimate HAWT fatigue damage from HAWT output data and mechanical components parameters using the Palmgren-Miner linear damage rule [10], [27]. The load signals must be first post-processed using the Downing-Socie RainFlow Counting (RFC) algorithm [28]. The algorithm counts the number of occurrences $n_{sk}(X_i, K_j)$ of load cycles s of amplitude L_{sk}, in the load history of the HAWT component k in closed loop with controller K_j under wind X_i. Interested readers can find a detailed description of RFC algorithm in [28]. To compute the component k damage denoted by $D_k(X_i, K_j)$, the Palmgrem-Miner rule is applied:

$$D_k(X_i, K_j) = \sum_{s=1}^{N} \frac{n_{sk}(X_i, K_j)}{N_k(L_{sk}(X_i, K_j))} \quad (5)$$

TABLE III: Considered components and their corresponding Replacement Costs (RC).

Component	RC (k$)
Blade	122
Hub	130
Blade pitch actuator	39
Rotor shaft	15
Gearbox	375
Tower	473

where N is the number of different kinds of cycles counted in the RFC algorithm, N_k is a function of the load cycle amplitude, yielding the number of cycles of amplitude L_{sk} that the component k can endure during its lifetime. It should be noticed that RFC can not be turned into a simple mathematical function [13] and is discontinuous, which makes it hard to consider damage directly as an objective function in classical optimal control designs [11], [13].

2) Cost function expression: To get an economic estimation of the HAWT fatigue cost during a simulation, the Replacement Cost (RC) of the considered components are estimated as in [29], with additional assumptions on transportation and installation costs. It is assumed that transportation and installation costs of each component are ratios of cost of the whole turbine, and that the larger and heavier the component is, the larger the ratio is. The considered components are the three blades, the hub, the three blade pitch actuators, the rotor shaft, the gearbox and the tower. A rough estimation of the RC of each component is summarized in Table III and is used for this application.

As mentioned in [30], the CPC power regulation is not affected by the IPC regulation. As only the IPC parameters are modified in the sequel, generated power would act as an offset, therefore only the cost related to the HAWT damage is considered in the fatigue cost. The HAWT fatigue cost is computed as follows:

$$\mathcal{Y}(X_i, K_j) = \sum_{k=1}^{10} \pi_k D_k(X_i, K_j) \tag{6}$$

where π_k refers to the RC of the k^{th} component. The target values mapping $\mathcal{Y}$ can thus be computed to fit the surrogate model f.

E. Surrogate model design

To design the surrogate model f, several strategies have been tested. The strategy showing the better results is described here. It aims at transforming the input and output data, in order to have a linear relation between the transformed inputs and outputs.

1) Outputs transformation: Empirically, $D \propto L^{m_k}$ where D is the damage, L is the load cycle amplitude and m_k is the Wöhler exponent of the component k material ($m_k = 4$ for steel and $m_k = 10$ for glass fiber). This causes the fatigue based cost function to have a log-normal, Rayleigh or Poisson distribution, as can be seen in Fig. 3. The Box-Cox

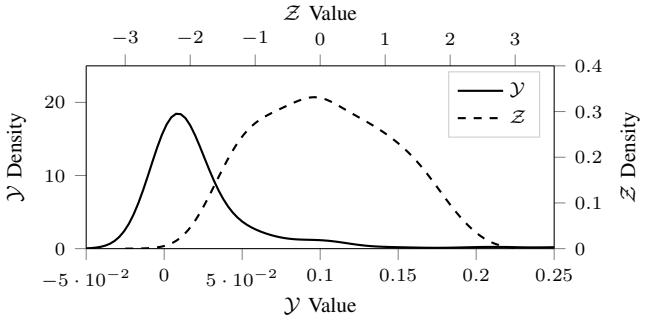

Fig. 3: Gaussian kernel density estimation of the distribution of fatigue cost $\mathcal{Y}$ (solid line), and fatigue cost after the Box-Cox transformation $\mathcal{Z}$ (dashed line).

transformation (7) transforms the log-normally distributed mapping $\mathcal{Y}$ to a quasi-normally distributed mapping $\mathcal{Z}$ [31].

$$z_{ij} = \frac{1}{\lambda}\left(y_{ij}^{\lambda} - 1\right) \tag{7}$$

In (7), $\lambda \in \mathbb{R}^*$ is the Box-Cox transformation parameter, $y_{ij} = \mathcal{Y}(X_i, K_j)$, z_{ij} corresponds to y_{ij} transformed in the log-normally distributed mapping $\mathcal{Z}$, such that $\mathcal{Z}(X_i, K_j) = z_{ij}$. Moreover, from aerodynamics theory, nonlinear relations between fluids and steady loads exist. Thus, it is easier to relate wind to a cost function scaled on loads rather than damage units. Hence the fatigue cost function is scaled on damage units. Using the Box-Cox transformation with $\frac{1}{\lambda}$ in the order of magnitude of m_k, it is possible to cancel the Wöhler exponent effects, causing the new mapping $\mathcal{Z}$ to be quasi-scaled on fatigue loads units.

2) Inputs transformation: As mentioned previously, steady aerodynamic loads are nonlinearly related to wind speed. Therefore, a polynomial features augmentation of degree 2 transforms the feature space $\mathcal{X}$ to a new feature space of higher dimension denoted by $\mathcal{X}_{aug}$. This is done by considering cross products of $\mathcal{X}$ components up to degree 2 as $\mathcal{X}_{aug}$ features. Thanks to this transformation, the relation between $\mathcal{X}$ and $\mathcal{Z}$, which is a curvy surface, becomes a hyperplane between $\mathcal{X}_{aug}$ and $\mathcal{Z}$, thus a linear regression is applied.

3) Linear regression: Eventually, ridge regression is used for predicting $\hat{z}_{ij}$ from $X_{i,aug}$ (8), which is the vector sample X_i in the augmented feature space $\mathcal{X}_{aug}$:

$$v_j^* = \underset{v_j}{\operatorname{argmin}} \left(\sum_i (v_j^T X_{i,aug} - z_{ij})^2 + C||v_j||_2^2\right) \tag{8a}$$

$$\hat{z}_{ij} = v_j^{*T} X_{i,aug} \tag{8b}$$

where C is a regularization parameter to control overfitting, $||.||_2$ is the L_2 norm, v_j and v_j^* are vectors. It should be noticed that v_j^* is the normal vector of the fitted hyperplane. The fatigue cost of controller K_j under the wind X_i, $\hat{y}_{ij} = f(X_i, K_j)$ can be predicted with the following procedure:

$$X_i \xrightarrow{\text{Poly. Aug.}} X_{i,aug} \xrightarrow{\text{Ridge Reg.}} \hat{z}_{ij} \xrightarrow{\text{Box Cox}^{-1}} \hat{y}_{ij}$$

IV. RESULTS

This section presents the preliminary results validating the approach. Metrics for the evaluation of each regression quality are first defined and there the results are presented.

A typical metric to assess regression quality is the R^2 score, expressed as follows:

$$R^2 = 1 - \frac{||y - \hat{y}||_2^2}{||y||_2^2} \tag{9}$$

where y and $\hat{y}$ are vectors of target and predicted values respectively. To assess not only prediction quality, but also the ability of the framework to reduce fatigue cost compared to a single controller K, the R_{dec} score is introduced as an additional metric:

$$\mathcal{C}(K) = \sum_i \mathcal{Y}(X_i, K) \tag{10a}$$

$$\hat{\mathcal{C}}(f, \mathcal{K}_{\text{list}}) = \sum_i \mathcal{Y}\left(X_i, K^*(X_i, f, \mathcal{K}_{\text{list}})\right) \tag{10b}$$

$$R_{\text{dec}}(K, f, \mathcal{K}_{\text{list}}) = 1 - \frac{\hat{\mathcal{C}}(f, \mathcal{K}_{\text{list}})}{\mathcal{C}(K)} \tag{10c}$$

where K^* is the controller selected by the method as explained in Section II. $\mathcal{C}(K)$ is the cumulative fatigue that would be obtained using the single controller K. $\hat{\mathcal{C}}(f, \mathcal{K}_{\text{list}})$ is the cumulative fatigue that would be obtained by selecting the controller $K^* \in \mathcal{K}_{\text{list}}$ minimizing the surrogate model f predictions. $R_{\text{dec}}(K, f, \mathcal{K}_{\text{list}})$ gives an image of the relative fatigue cost reduction which could be achieved using the surrogate model and the set of controllers $\mathcal{K}_{\text{list}}$ with respect to a single controller K, in spite of prediction errors. Note that R_{dec} is computed neglecting LiDAR limitations and additional switch transient fatigue cost. To understand the sensitivity of fatigue reduction to the surrogate model fitting quality, R_{dec} must be compared to the R_{dec} score using a fictitious surrogate model f^{id} which would give perfect predictions. This R_{dec} score with an ideal surrogate model is denoted by $R_{\text{dec}}^{\text{id}}$. Hence, $f^{\text{id}}(X_i, K_j) = \mathcal{Y}(X_i, K_j)$, f^{id} R^2 score is 1 and $R_{\text{dec}}^{\text{id}}(K, \mathcal{K}_{\text{list}}) = R_{\text{dec}}(K, f^{\text{id}}, \mathcal{K}_{\text{list}})$.

Simulations of 600 seconds are taken into account during the data generation process. In order to ensure that no transient is still present during cost function evaluation, only the last 300 seconds are used for this purpose.

After the post-processing of the simulations with the fatigue based cost function, it was observed that in more than 90% of the simulations, one of the four controllers, whose parameters are summarized in Table IV, could be found among the top ten of the controllers giving the lowest fatigue cost. Therefore to make the results analysis more tractable, only these four controllers were retained.

A regression of each controller fatigue cost against the wind features, using the strategy presented in Section III-E is fitted. A training set of 294 winds is drawn from $\mathcal{X}$. The algorithm is fitted on the training set, and tested on its complement.

TABLE IV: Summary of selected controllers gains.

Controller	K_P	K_I
1	4×10^{-5}	3.2889×10^{-5}
2	4×10^{-5}	5.1556×10^{-5}
3	0.0086	0.0031
4	0.0186	0.0066

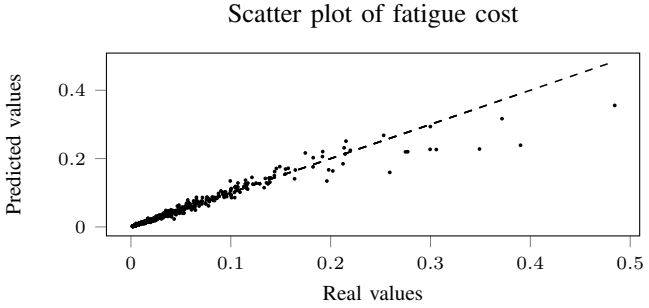

Fig. 4: Scatter plot on 294 unseen winds and 5 different controllers, the black dashed line represents the perfect predictions.

The only tuning parameter of the surrogate model is the regularization parameter C of the Ridge regression. This parameter was chosen to maximize the R^2 score through grid searching.

The R^2 and R_{dec} scores on the test set are summarized in Table V. The R^2 scores are satisfactory, above 0.9. The R_{dec} score, which reflects the relative fatigue cost decrease from a candidate controller, reaches 21% with the best controller in $\mathcal{K}_{\text{list}}$, out of the 23% which could be expected if the predictions were perfect. These scores depend on the drawn set, but R_{dec} and $R_{\text{dec}}^{\text{id}}$ scores for the best candidate controller are always between 15% and 25%. However, it should be noticed that R_{dec} scores, which reflect the expected fatigue reduction, are very high and this is related to the set of winds considered. This set was made of strong winds, the occurrence probability of which is quite low. For a realistic wind distribution, such high fatigue costs should be more rare and therefore the R_{dec} scores should be reduced.

The regression quality with the 4 controllers and the 294 test winds can be seen in Fig. 4. One can see that the prediction error increases with the predicted value, which is a well-known behavior of the Box-Cox transformation. Linear regression minimizes the square of prediction error on the $\mathcal{Z}$ mapping, but the inverse Box-Cox transformation distorts $\mathcal{Y}$, then the regression becomes more sensitive to prediction errors for high values.

TABLE V: R^2, R_{dec} and $R_{\text{dec}}^{\text{id}}$ scores for each controller.

Controller	R^2	R_{dec}	$R_{\text{dec}}^{\text{id}}$
1	0.95	30%	31%
2	0.96	29%	31%
3	0.96	26%	28%
4	0.93	21%	23%

V. CONCLUSION AND PERSPECTIVES

This paper presents an innovative data-driven framework for the on-line fatigue based selection of a controller among a discrete set of candidates. Firstly, an economic fatigue based cost function accounting for closed loop HAWT operational cost was established. Secondly, a regression from turbulent spectrum wind features to the fatigue cost function, has been derived for each candidate controller, giving R^2 scores above 0.9. Thirdly, the fatigue cost prediction for each controller has shown a great potential in selecting the candidate controller that minimizes HAWT fatigue cost. This method would allow fatigue cost reduction up to 21% from the best candidate alone for the considered wind distribution. This is accomplished without considering additional fatigue cost due to possible transients following wind changes and with perfect knowledge of the future turbulent wind spectrum. The quantification of the fatigue cost reduction on realistic wind distributions is in the scope of future works, as well as a more realistic validation including the switch between controllers on an aero-elastic simulator.

The main advantages of this approach are to limit controller tuning procedure sensitivities and to provide a data-driven fatigue-based control strategy, that can be effectively adapted to different HAWT systems.

In the presented application, a discrete set of PI controllers is considered, but the extension of this method to a set of candidates with different advanced control techniques, or a continuum of PI controllers, is possible. By taking the controller showing the greatest potential in the current wind conditions, it could be possible to achieve convenient controller performance regarding a complex cost function, using simple controller designs. Finally, the surrogate model performance could be improved using more complex designs such as neural networks or gaussian processes and/or adding other features allowing to better explain the HAWT closed loop performance.

REFERENCES

[1] G. W. E. Council, "Global wind report," *GWEC, Brussels, Belgium, Technical Report*, 2017.

[2] G. W. E. Council, "Global wind energy outlook," *GWEC, Brussels, Belgium, Technical Report*, 2016.

[3] M. O. Hansen, *Aerodynamics of wind turbines*. Routledge, 2015.

[4] E. Bossanyi, "Individual blade pitch control for load reduction," *Wind Energy*, vol. 6, no. 2, pp. 119–128, 2003.

[5] D. Schlipf, S. Schuler, P. Grau, F. Allgöwer, and M. Kühn, "Look-ahead cyclic pitch control using LiDAR," in *Proc. The Science of Making Torque from Wind*, 2010.

[6] M. Mirzaei, M. Soltani, N. K. Poulsen, and H. H. Niemann, "An MPC approach to individual pitch control of wind turbines using uncertain LiDAR measurements," in *Proc. European Control Conference (ECC)*, pp. 490–495, IEEE, 2013.

[7] S. Raach, D. Schlipf, F. Sandner, D. Matha, and P. W. Cheng, "Nonlinear model predictive control of floating wind turbines with individual pitch control," in *Proc. American Control Conference (ACC)*, pp. 4434–4439, IEEE, 2014.

[8] Z. Civelek, M. Lüy, E. Çam, and H. Mamur, "A new fuzzy logic proportional controller approach applied to individual pitch angle for wind turbine load mitigation," *Renewable Energy*, vol. 111, pp. 708–717, 2017.

[9] D. Ossmann, J. Theis, and P. Seiler, "Load reduction on a clipper liberty wind turbine with linear parameter-varying individual blade pitch control," *Wind Energy*, vol. 20, no. 10, pp. 1771–1786, 2017.

[10] A. Palmgren, "Die lebensdauer von kugellagern. z. vdi 68," *S339–S341*, 1924.

[11] K. Hammerum, P. Brath, and N. K. Poulsen, "A fatigue approach to wind turbine control," in *Journal of Physics: Conference Series*, vol. 75, p. 012081, IOP Publishing, 2007.

[12] J. Barradas-Berglind and R. Wisniewski, "Representation of fatigue for wind turbine control," *Wind Energy*, vol. 19, no. 12, pp. 2189–2203, 2016.

[13] T. Knudsen, T. Bak, and M. Svenstrup, "Survey of wind farm control—power and fatigue optimization," *Wind Energy*, vol. 18, no. 8, pp. 1333–1351, 2015.

[14] I. Van der Hoven, "Power spectrum of horizontal wind speed in the frequency range from 0.0007 to 900 cycles per hour," *Journal of meteorology*, vol. 14, no. 2, pp. 160–164, 1957.

[15] A. Clifton, S. Schreck, G. Scott, N. Kelley, and J. K. Lundquist, "Turbine inflow characterization at the national wind technology center," *Journal of Solar Energy Engineering*, vol. 135, no. 3, p. 031017, 2013.

[16] F. Guillemin, H.-N. Nguyen, G. Sabiron, D. Di Domenico, and M. Boquet, "Real-time three dimensional wind field reconstruction from nacelle LiDAR measurements," in *Journal of Physics: Conference Series*, vol. 1037, p. 032037, IOP Publishing, 2018.

[17] H. S. Toft, L. Svenningsen, W. Moser, J. D. Sørensen, and M. L. Thøgersen, "Wind climate parameters for wind turbine fatigue load assessment," *Journal of Solar Energy Engineering*, vol. 138, no. 3, p. 031010, 2016.

[18] I. Abdallah, A. Natarajan, and J. D. Sørensen, "Influence of the control system on wind turbine loads during power production in extreme turbulence: Structural reliability," *Renewable Energy*, vol. 87, pp. 464–477, 2016.

[19] J. P. Murcia, P.-E. Réthoré, N. Dimitrov, A. Natarajan, J. D. Sørensen, P. Graf, and T. Kim, "Uncertainty propagation through an aeroelastic wind turbine model using polynomial surrogates," *Renewable Energy*, vol. 119, pp. 910–922, 2018.

[20] N. Dimitrov, M. Kelly, A. Vignaroli, and J. Berg, "From wind to loads: wind turbine site-specific load estimation using databases with high-fidelity load simulations," *Wind Energ. Sci. Discuss*, 2018.

[21] L. Schröder, N. K. Dimitrov, D. R. Verelst, and J. A. Sørensen, "Wind turbine site-specific load estimation using artificial neural networks calibrated by means of high-fidelity load simulations," in *Journal of Physics: Conference Series*, vol. 1037, p. 062027, IOP Publishing, 2018.

[22] J. M. Jonkman *et al.*, "Dynamics modeling and loads analysis of an offshore floating wind turbine," *National Renewable Energy Laboratory*, 2007.

[23] R. P. Coleman and A. M. Feingold, "Theory of self-excited mechanical oscillations of helicopter rotors with hinged blades," 1957.

[24] J. Jonkman and B. Jonkman, "NWTC information portal (FAST v8) https://nwtc.nrel.gov," 2016.

[25] N. Kelley and B. Jonkman, "NWTC computer-aided engineering tools (turbsim)," *Last Modified*, vol. 442, 2013.

[26] I. E. Commission *et al.*, "IEC 61400-1: Wind turbine generator systems-part 1: Safety requirements," *International Standard*, pp. 1400–1, 1999.

[27] M. Miner, "Cumulative damage in fatigue journal of applied mechanics 12 (1945) no. 3, pp," *A159-A164*, 1945.

[28] S. D. Downing and D. Socie, "Simple rainflow counting algorithms," *International journal of fatigue*, vol. 4, no. 1, pp. 31–40, 1982.

[29] L. J. Fingersh, M. M. Hand, and A. S. Laxson, "Wind turbine design cost and scaling model," 2006.

[30] T. Burton, N. Jenkins, D. Sharpe, and E. Bossanyi, *Wind energy handbook*. John Wiley & Sons, 2011.

[31] G. E. Box and D. R. Cox, "An analysis of transformations," *Journal of the Royal Statistical Society. Series B (Methodological)*, pp. 211–252, 1964.